

Validation of dynamic models to predict flux decline in the ultrafiltration of macromolecules

M. Cinta Vincent Vela^{a*}, Enrique Bergantiños Rodríguez^b, Silvia Álvarez Blanco^a,
Jaime Lora García^a

^a*Chemical and Nuclear Engineering Department, Polytechnic University of Valencia,
C/Camino de Vera s/n 46022 Valencia, Spain*

Tel. +34 (96) 387-7000, ext. 76383; Fax. +34 (96) 387-7639; email: mavinve@iqn.upv.es

^b*Chemical Engineering Department, Polytechnical Institute José A. Echeverría, Ave. 114, No. 11901, Havana, Cuba*

Received 29 January 2006; Accepted 15 March 2006

Abstract

The aim of this work was to validate the dynamic model for the average permeate flux that considers membrane fouling as a dynamic process from non-equilibrium to equilibrium to predict permeate flux decline with time in the ultrafiltration of macromolecules. This is one of the most accepted ultrafiltration dynamic models and it considers cake formation as the main fouling mechanism. For this purpose, several experiments were performed at pilot plant scale and the results were compared with the ones predicted by the model. A ceramic TiO₂-Al₂O₃ monotubular membrane (Tami, S.A., France) of 5 kDa molecular weight cut-off was used. Aqueous solutions with different concentrations of polyethylene glycol were used as feed. The flow rate and the transmembrane pressure were varied while the temperature was maintained constant at 25°C. As the model does not consider cake compaction, the best results were obtained for low transmembrane pressures, as expected. Crossflow velocity was observed to be one of the main factors affecting fouling. The best agreement between the experimental results and those predicted by the model was obtained for low crossflow velocities as cake formation can be considered as the main fouling mechanism in this case.

Keywords: Permeate flux; Fouling; Ultrafiltration; Macromolecules; Dynamic model

*Corresponding author.

Presented at the EuroMed 2006 conference on Desalination Strategies in South Mediterranean Countries: Cooperation between Mediterranean Countries of Europe and the Southern Rim of the Mediterranean. Sponsored by the European Desalination Society and the University of Montpellier II, Montpellier, France, 21–25 May 2006.

0011-9164/07/\$– See front matter © 2007 Elsevier B.V. All rights reserved

1. Introduction

Fouling is a major drawback in membrane processes. It causes a severe decrease in the permeability of the membrane. Two fundamental mechanisms are responsible for flux decline [1]: pore blocking and cake formation. Pore blocking can occur on the membrane surface or inside the pores. The rapid initial flux decline is attributed to the instantaneous pore blocking of some of the membrane pores [2]. Membrane pore blocking is favoured when the solute molecules and the membrane pores are similar in size [3], although molecular aggregation and deformation can have a notorious influence. A cake layer is formed on the membrane surface when the adequate combination of operating parameters (transmembrane pressure (TMP), crossflow velocity, etc.) and solution characteristics (concentration, viscosity, etc.) cause it to form. High values of TMP, viscosity and concentration and low values of crossflow velocity usually facilitate the development of the cake layer.

Modelling of flux decline with time can help to understand the fouling phenomenon and to prevent it. In the last 15 years numerous advances have been achieved in the understanding and modelling of the fouling phenomenon that causes flux decline in micro and ultrafiltration (UF) processes. However, the mechanisms of fouling, the variables that may have an influence on fouling and their interrelation are still a field with high expectations and insufficient results.

The first models proposed to predict permeate flux decline were obtained from conventional filtration theory [4]. These models are empirical and they predict a continuous flux decline until a value of zero.

Other dynamic models for UF were formulated later. Some of them are adaptations to cross-flow UF of models that were developed for dead-end UF [5]. Others consider gel formation as the main fouling mechanism [6–8]. There are some models that combine several fouling mechanisms:

osmotic pressure and cake formation [9], pore blocking and cake formation [10], etc.

In this work, the experimental values of permeate flux obtained under different operating conditions were compared with the results predicted by the dynamic model for the average permeate flux that considers membrane fouling as a dynamic process from non-equilibrium to equilibrium, which is one of the most accepted UF dynamic models [11].

2. Theoretical

The dynamic model for the average permeate flux that considers membrane fouling as a dynamic process from non-equilibrium to equilibrium [11] regards cake formation as the main fouling mechanism. Two different regions over the membrane surface are considered. One of them is close to the feed inlet where the gel layer is formed instantly and the steady-state is achieved first. The other one is a non-stationary zone that becomes stationary after a certain time. There is a frontier between the two regions that moves along the membrane separating the stationary region and the non-stationary region. The equation to estimate the value of permeate flux all over the membrane [Eq. (6)] can be obtained as a function of the frontier position and the value of the permeate flux in each region.

The filtration number (N_F) relates the energy needed for the transportation of a molecule from the membrane surface to the bulk solution with the dissipative energy of the molecule. This dimensionless parameter can be calculated as follows [Eq. (1)]:

$$N_F = \frac{4\pi a_p^3}{3kT} \Delta P_{pc} \quad (1)$$

where a_p is the radius of the solute molecule, k is the Boltzman constant, T is the absolute tem-

perature and P_{pc} is the pressure loss across the concentration polarization layer.

The pressure loss in the concentration polarization layer can reach a maximum critical value above which the gel layer begins to form. When this critical pressure, P_c , is considered, the so-called critical filtration number, N_{FC} , is calculated as follows [6]:

$$N_{FC} = \int_0^{\theta_{GV}} \frac{1 + \frac{2}{3}\theta^5}{1 - \frac{3}{2}\theta + \frac{3}{2}\theta^5 - \theta^6} 3\theta^2 d\theta \quad (2)$$

with $\theta = C_v$, C_v being the solute concentration in volume fraction and the sub-index *GV* referring to the gel layer.

The permeate flux in the no stationary region, $J(t)$, is described by Eq. (3):

$$J(t) = \frac{(\Delta P - \Delta P_c)}{\mu R_m} \left[1 + \frac{2 r_c (\Delta P - \Delta P_c) C_0}{\mu^2 R_m^2 C_g} t \right]^{-1/2} \quad (3)$$

where ΔP is the transmembrane pressure, μ is the dynamic viscosity of the permeate, R_m is the membrane hydraulic resistance, r_c is the specific resistance of the gel layer, C_0 is the feed concentration, C_g is the gel layer concentration and t is time.

The cake thickness in the non-stationary region, $\delta(t)$, is inversely related to the local permeate flux, $J(t)$ [Eq. (4)].

$$\delta(t) = \frac{(\Delta P - \Delta P_c)}{r_c J(t)} - \frac{R_m}{r_c} \quad (4)$$

The frontier position, $x(t)$, between the stationary and the non-stationary region, is given by Eq. (5):

$$x(t) = 4.81 (D^2 \gamma) \left(\frac{C_0}{C_g} \right)^{1/2} \left(\frac{r_c}{\Delta P - \Delta P_c} t \right)^{3/2} \quad (5)$$

where D is the diffusivity and γ is the shear rate, which is given by Eq. (6).

$$\gamma = 8 \frac{v_{\text{tang}}}{D_{\text{int}}} \quad (6)$$

where v_{tang} is the crossflow velocity and D_{int} is the internal diameter of the membrane.

The permeate flux all over the membrane can be estimated by Eq. (7):

$$J(t) = \frac{1.31}{L} \left[\frac{C_g D^2 \gamma}{C_0} x(t)^2 \right]^{1/3} + \frac{L - x(t)}{L} J(t) \quad (7)$$

where L is the membrane length.

When $x(t) = L$, the limiting flux, J_{lim} , is reached.

$$J_{\text{lim}} = 1.31 \left[\frac{C_g D^2 \gamma}{C_0 L} \right]^{1/3} \quad (8)$$

3. Materials and methods

3.1. Membrane characteristics

The membrane used in the experiments was a ceramic $\text{TiO}_2\text{-Al}_2\text{O}_3$ monotubular membrane (Tami, S.A., France) with a molecular weight cut-off (MWCO) of 5 kDa, an internal diameter of 6 mm and an active surface of 35.5 cm².

3.2. Feed solution

The feed solution was an aqueous solution of polyethylene glycol (PEG) with a molecular weight of 35,000 g/mol. Different PEG concentrations were considered: 5, 10 and 15 g/L. The PEG used was supplied by Merck-Schuchardt

(Germany). Deionized water was used to prepare the solutions.

3.3. Cleaning solution

The cleaning solution was 250 ppm of NaClO. To prevent steel corrosion NaOH was added until a pH value of 11 was reached. NaOH pellets and NaClO of 10% (w/v) were supplied by Panreac (Spain).

3.4. Analytical methods

Feed and permeate concentration were measured with chemical oxygen demand (COD) cell tests provided by Merck (Germany) for 25–1500 ppm and 500–10,000 ppm. The procedure was analogous to that described in EPA 410.4, US Standard Methods 5220 D and ISO 15705.

3.5. Experiments

The UF equipment used was described elsewhere [12]. The flow rate varied between 1 and 3 m/s and TMP between 0.2 and 0.5 MPa. The temperature was set constant at 25°C. Experiments at different feed concentrations (5, 10 and 15 g/L) were carried out to estimate the gel layer concentration. The membrane was cleaned after each experiment. It was first rinsed with deionized water for 30 min, then cleaned with a NaClO–NaOH solution for 60 min and finally it was rinsed again with deionized water for 30 min. All the cleaning steps were carried out at 40°C and TMP close to zero. Membrane permeability was totally recovered after the cleaning cycle.

4. Results and discussion

4.1. Estimation of model parameters

The specific resistance of the cake layer was calculated taking into account the Carman–Kozeny equation [Eq. (9)] where ϵ is the cake

porosity [3,5,11]:

$$r_c = \frac{45 \cdot \mu \cdot (1 - \epsilon)^2}{a^2 \cdot \epsilon^3} \quad \epsilon = 1 - C_{GV} \quad (9)$$

The Stokes–Einstein radius of PEG as a function of its molecular weight (MW) was estimated by means of Eq. (10) [13]. All the variables in Eq. (10) are expressed in the international system of units (SI).

$$a_p = \left[0.262 \cdot (\text{MW})^{0.5} - 0.3 \right] \cdot 10^{-10} \quad (10)$$

Eq. (10) is valid for a MW range of 200–40,000 g/mol and has been very often used [14,15].

The gel layer concentration estimated from the experimental results obtained under the most critical operating conditions for the cake layer to form: the highest TMP and the highest feed concentration (0.5 MPa and 15 g/L) is shown in Table 1. The equation proposed by Lee et al. was employed [16]. That equation can be used in the case of tubular membranes and turbulent flow. It was found that the gel layer concentration varied slightly with the crossflow velocity (Table 1). The diffusivity of PEG at 25°C can be correlated with the MW of the molecule by means of the following equation [17,18]:

$$D = 9.82 \cdot 10^{-9} \cdot (\text{MW})^{-0.52} \quad (11)$$

Table 1
Gel layer concentration as a function of crossflow velocity

| Crossflow velocity (m/s) | Gel layer concentration (g/L) |
|--------------------------|-------------------------------|
| 1 | 24.86 |
| 2 | 25.15 |
| 3 | 24.04 |

In the literature other correlations can be found for the diffusivity of PEG as a function of the MW [19–21], but they are less accurate.

4.2. Comparison of experimental results and results predicted by the model

The results predicted by the model were compared with the experimental results in Figs. 1–3. The symbols correspond to the experimental data on permeate flux vs. time and the continuous lines correspond to the model predictions.

The experimental results did not show the rapid initial flux decline that corresponds to pore blocking [2]. However, permeate flux remained approximately constant from the beginning. This can be due to the large difference between the MW of the solute, 35 kg/mol, and the membrane MWCO, which was 5 kDa. For this reason pore blocking was not very likely to occur in the fouling experiments and flux decline can be attributed mainly to concentration polarization and cake formation.

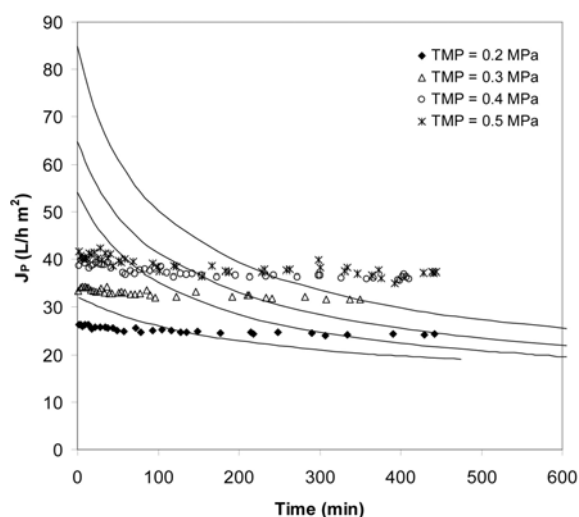


Fig. 1. Comparison between experimental results and permeate fluxes predicted by the model at a crossflow velocity of 1 m/s and a feed concentration of 5 g/L.

Cake formation is the main fouling mechanism considered by the model used in this work. Crossflow velocity was observed to be one of the main factors affecting fouling. The best agreement between the experimental results and those predicted by the model was obtained for low crossflow velocities as cake formation can be considered as the main fouling mechanism in this case. For higher crossflow velocities, 2 and 3 m/s (Figs. 2 and 3), the experimental results differ more from the data predicted by the model because the tendency of solute molecules to form a gel layer decreases.

As can be seen in Fig. 1, the differences between experimental and predicted results are more notorious for short time scales, being permeate flux over predicted in all cases (Figs. 1–3). This can be attributed to the fact that the model considers concentration polarization as the main mechanism responsible for flux decline in the early stages of the UF process. However, cake formation can be present in the very early beginnings of UF.

For all crossflow velocities (Figs. 1–3) experimental and predicted results are closer for lower

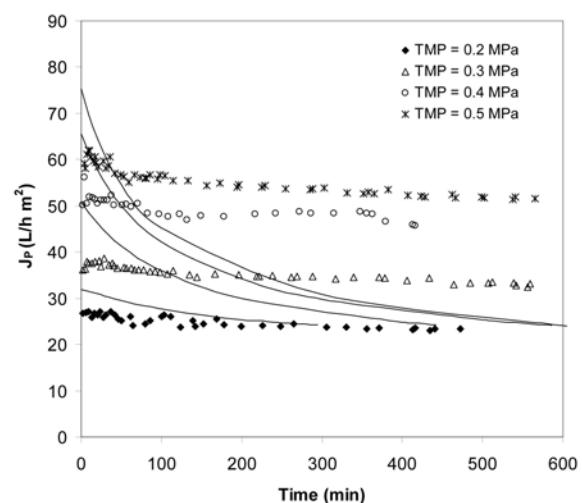


Fig. 2. Comparison between experimental results and permeate fluxes predicted by the model at a crossflow velocity of 2 m/s and a feed concentration of 5 g/L.

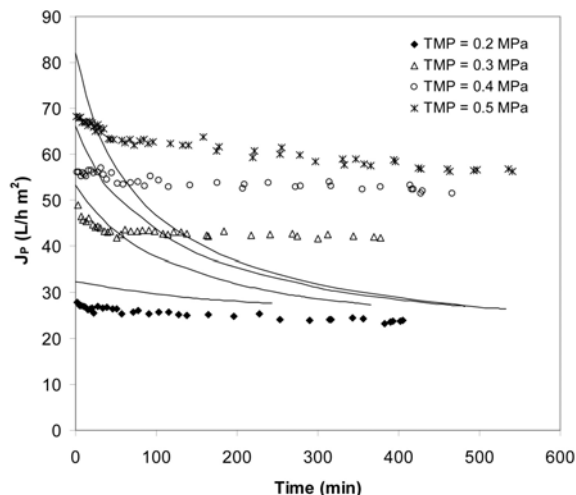


Fig. 3. Comparison between experimental results and permeate fluxes predicted by the model at a crossflow velocity of 3 m/s and a feed concentration of 5 g/L.

TMPs. The reason for this may be that the model predicts an increase in the cake layer thickness with TMP, which can be observed when substituting Eq. (3) in Eq. (4). That may cause greater flux decline than the one that could occur if the cake layer thickness did not increase with TMP. As TMP increases, the model predicts a higher cake thickness than the one experimentally obtained. Because of this, the model predicts lower steady-state permeate fluxes for high TMPs than the experimentally observed ones.

The model predicts a limiting permeate flux inferior to the stationary values experimentally obtained (Figs. 1–3), and it is also achieved later than experimentally observed. The consolidation of the gel layer occurs earlier in the experiments than in the results predicted by the model.

The time needed to achieve steady-state permeate flux experimentally was observed to increase with TMP. This can be observed in Figs. 1–3 and can be due to the increase in the gel layer thickness with pressure. The model also predicts an increase in the time needed to achieve a steady-state permeate flux with TMP.

5. Conclusions

The model can only partially predict the experimental results obtained in this work. The model predicts flux decline in an UF process that ends up in a limiting flux and a consolidated gel layer. These conditions may only be achieved for low crossflow velocities (1 m/s). For this crossflow velocity, predicted and experimental results were observed to be more similar.

The model predicts lower changes in permeate flux with crossflow velocity than those experimentally observed. The sensibility of the model to the gel layer concentration value is very high. Taking into account the existing theoretical and practical deficiencies in the estimation of the gel layer concentration, the applicability of this model is limited.

6. Symbols

| | |
|-----------------|--|
| a_p | — Radius of the PEG molecule, m |
| C_g | — Gel concentration, kg/m ³ |
| C_{GV} | — Gel concentration, v/v |
| C_0 | — Feed concentration, kg/m ³ |
| C_v | — Solute concentration, v/v |
| D | — Solute diffusivity, m ² /s |
| D_{int} | — Internal diameter of the membrane, m |
| J_{lim} | — Limiting permeate flux, m/s) |
| $J(t)$ | — Permeate flux in the non-stationary region, m/s |
| k | — Boltzman's constant, J/K |
| L | — Membrane length, m |
| N_F | — Filtration number |
| N_{Fc} | — Critical filtration number |
| ΔP | — Transmembrane pressure, Pa |
| ΔP_c | — Critical pressure, Pa |
| ΔP_{cp} | — Pressure loss due to concentration polarization layer, Pa |
| r_c | — Specific resistance of the cake layer, kg/m ³ s |
| R_m | — Membrane hydraulic resistance, m ⁻¹ |

t — Time, s
 T — Temperature, K
 v_{tang} — Crossflow velocity, m/s
 $x(t)$ — Frontier position, m

Greek

$\delta(t)$ — Cake thickness, m
 γ — Shear rate, s^{-1}
 ε — Cake porosity
 μ — Dynamic viscosity, kg/m/s

References

- [1] L. Song, *J. Coll. Interf. Sci.*, 214 (1999) 251–263.
 [2] K. Stamatakis and C. Tien, *Amer. Inst. Chem. Eng. J.*, 39 (1993) 1292–1302.
 [3] G. Belfort, R.H. Davis and A.L. Zydney, *J. Membr. Sci.*, 96 (1994) 1–58.
 [4] J. Hermia, *Trans. Inst. Chem. Eng.*, 60 (1982) 183–187.
 [5] R.H. Davis, *Sep. Purif. Methods*, 21 (1992) 75–126.
 [6] L. Song, *J. Membr. Sci.*, 144 (1998) 173–185.
 [7] L. Wang and L. Song, *J. Membr. Sci.*, 160 (1999) 41–50.
 [8] N. Mugnier, J.A. Howell and M. Ruf, *J. Membr. Sci.*, 175 (2000) 149–161.
 [9] S. Bhattacharjee and P.K. Bhattacharya, *J. Membr. Sci.*, 72 (1992) 149–161.
 [10] C.-C. Ho and A.L. Zydney, *J. Coll. Interf. Sci.*, 232 (2000) 389–399.
 [11] L. Song, *J. Membr. Sci.*, 139 (1998) 183–200.
 [12] M.C. Vincent-Vela, S. Álvarez-Blanco and J. Lora-García, *Desalination*, 184 (2005) 347–356.
 [13] C. Tam and A. Trembley, *J. Membr. Sci.*, 57 (1991) 271–287.
 [14] P. Puhlfürß, A. Voigt, R. Weber and M. Morbe, *J. Membr. Sci.*, 174 (2000) 123–133.
 [15] D. Möckel, E. Staude and M.D. Guiver, *J. Membr. Sci.*, 158 (1999) 63–75.
 [16] S. Lee, J. Kim and C.H. Lee, *J. Membr. Sci.*, 163 (1999) 63–74.
 [17] P. Prádanos, J.I. Arribas and A. Hernández, *J. Membr. Sci.*, 99 (1995) 1–20.
 [18] M. Cheryan, ed., *Ultrafiltration and Microfiltration Handbook*, 2nd ed., CRC Press, New York, 1998.
 [19] C. Bhattacharjee and S. Datta, *J. Membr. Sci.*, 119 (1996) 39–46.
 [20] S. Das Gupta and P.K. Bhattacharya, *Chem. Eng. Comm.*, 93 (1990) 193–210.
 [21] T.K. Sherwood, R.L. Pigford and C.R. Wilke, ed., *Mass Transfer*, McGraw Hill, New York, 1975.